THE JOURNAL OF BIOLOGICAL CHEMISTRY
Vol. 280, No. 9, Issue of March 4, pp. 7677–7684, 2005
Printed in U.S.A.
© 2005 by The American Society for Biochemistry and Molecular Biology, Inc.

Evidence for the Presence of Three Distinct Binding Sites for the Thioflavin T Class of Alzheimer's Disease PET Imaging Agents on β-Amyloid Peptide Fibrils*

Received for publication, October 25, 2004, and in revised form, December 14, 2004
Published, JBC Papers in Press, December 21, 2004, DOI 10.1074/jbc.M412056200

Andrew Lockhart‡§, Liang Ye‡, Duncan B. Judd¶, Andy T. Merritt¶, Peter N. Lowe‖, Jennifer L. Morgenstern‡, Guizhu Hong‡, Antony D. Gee‡, and John Brown‡

From the ‡Translational Medicine and Technology, GlaxoSmithKline Research and Development, Addenbrookes Hospital, Cambridge CB2 2GG and ¶High Throughput Chemistry and ‖Molecular Interactions, GlaxoSmithKline Research and Development, Medicine Research Centre, Gunnels Wood Road, Stevenage SG1 2NY, United Kingdom

Imaging the progression of Alzheimer's disease would greatly facilitate the discovery of therapeutics, and a wide range of ligands are currently under development for the detection of β-amyloid peptide (Aβ)-containing plaques by using positron emission tomography. Here we report an in-depth characterization of the binding of seven previously described ligands to *in vitro* generated Aβ-(1–40) polymers. All of the compounds were derived from the benzothiazole compound thioflavin T and include 2-[4′-(methylamino)phenyl]benzothiazole and 2-(4′-dimethylamino-)phenyl-imidazo[1,2-*a*]-pyridine derivatives, 2-[4′-(dimethylamino)phenyl]-6-iodobenzothiazole and 2-[4′-(4″-methylpiperazin-1-yl)phenyl]-6-iodobenzothiazole, and a benzofuran compound (5-bromo-2-(4-dimethylaminophenyl)benzofuran). By using a range of fluorescent and radioligand binding assays, we find that these compounds display a more complex binding pattern than described previously and are consistent with three classes of binding sites on the Aβ fibrils. All of the compounds bound with very high affinity (low nM K_d) to a low capacity site (BS3) (1 ligand-binding site per ~300 Aβ-(1–40) monomers) consistent with the previously recognized binding site for these compounds on the fibrils. However, the compounds also bound with high affinity (K_d ~100 nM) to either one of two additional binding sites on the Aβ-(1–40) polymer. The properties of these sites, BS1 and BS2, suggest they are adjacent or partially overlapping and have a higher capacity than BS3, occurring every ~35 or every ~4 monomers of Aβ-(1–40)-peptide, respectively. Compounds appear to display selectivity for BS2 based on the presence of a halogen substitution (2-[4′-(dimethylamino)phenyl]-6-iodobenzothiazole, 2-[4′-(4″-methylpiperazin-1-yl)phenyl]-6-iodobenzothiazole, and 5-bromo-2-(4-dimethylaminophenyl)benzofuran) on their aromatic ring system. The presence of additional ligand-binding sites presents potential new targets for ligand development and may allow a more complete modeling of the current positron emission tomography data.

Alzheimer's disease (AD)[1] is a common neurological disease of chronic dementia, memory loss, and cognitive impairment. Central to the neuropathology of AD is the deposition in specific brain regions of polymeric peptide/protein deposits, composed of β-amyloid peptide (Aβ) and tau protein, termed senile plaques (SPs) and neurofibrillary tangles (NFTs), respectively (reviewed in Ref. 1).

The precise role of these deposits in the pathogenesis of AD is still unclear. However, individuals with mutations leading to increased Aβ production are at a high risk of developing AD (2), and individuals with mutations in the tau gene are linked to a class of neurodegenerative diseases including frontotemporal dementia and parkinsonism linked to chromosome 17 (3). Moreover, the accumulation of SPs and NFTs follows a predictable temporal and spatial sequence in individuals affected with AD (4, 5). Detection of these deposits may therefore provide a clinically useful tool for monitoring disease progression and treatment effects. Positron emission tomography (PET) uses positron emitting radioligands to image and measure ligand-binding sites *in vivo* and is currently being developed as a sensitive way to track SPs and NFTs in patients (reviewed in Ref. 6).

Three broad categories of PET ligands of AD-associated polymers are currently under investigation. One class is derived from the dye thioflavin T (Thio T) and includes BTA/PIB (7, 8), IMPY (9), TZDM, and TZPI (10). A second class is characterized by a styrylbenzene backbone and includes X34 (11), X04 (12), IMSB (10), BSB (10), and the stilbenes (13). The final class has an aminonaphthyl core and includes FENE and FDDNP (14).

The binding of these compounds to Aβ-(1–40) fibrils generated *in vitro* has been investigated in a number of laboratories, and the results of these studies so far are consistent with three independent binding sites, one for each structural class of ligand, and all with high binding affinities. However, the binding stoichiometry for all these structural classes of ligand has been reported to be low, with ligand-binding sites occurring only every few hundreds (8) or even thousands (14) of Aβ-(1–40) monomers, and this raises a question of whether the signal to be anticipated from further development of these radioligands will be clinically useful.

Two of the ligands 6-OH-BTA-1/PIB and FDDNP have so far

* The costs of publication of this article were defrayed in part by the payment of page charges. This article must therefore be hereby marked "*advertisement*" in accordance with 18 U.S.C. Section 1734 solely to indicate this fact.

§ To whom correspondence should be addressed: GlaxoSmithKline, ACCI, Box 128, Addenbrookes Hospital, Hills Road, Cambridge CB2 2GG, UK. Tel.: 44-1223-296077; Fax: 44-1223-296063; E-mail: andrew.2.lockhart@gsk.com.

[1] The abbreviations used are: AD, Alzheimer's disease; Aβ, amyloid β-peptide; SP, senile plaque; NFT, neurofibrillary tangle; PET, positron emission tomography; FLINT, fluorescence intensity; FRET, fluorescence energy transfer; BP, binding potential; Thio T, thioflavin T; BTA-1, 2-[4′-(methylamino)phenyl]benzothiazole; 6-Me-BTA-1, 2-[4′-(methylamino)-phenyl]-6-methylbenzothiazole; IMPY-H, 2-(4′-dimethylamino-)phenyl-imidazo[1,2-*a*]-pyridine; IMPY-Me, 6-methyl-2-(4′-dimethylamino)-phenyl-imidazo[1,2-*a*]-pyridine; TZDM, 2-[4′-(dimethylamino)phenyl]-6-iodobenzothiazole; TZPI, 2-[4′-(4″-methylpiperazin-1-yl)phenyl]-6-iodobenzothiazole; BF1, 5-bromo-2-(4-dimethylaminophenyl)benzofuran; PIB, Pittsburgh compound B.

This is an Open Access article under the CC BY license.

progressed to *in vivo* imaging studies (15, 16), comparing small numbers of control and AD patients. The results demonstrate increased retention of labeled species in areas of the brain thought to be affected by AD. However, the precise nature of the signal in these studies remains uncertain given the low density of ligand-binding sites apparently present on Aβ fibrils. The situation is further complicated by *ex vivo* measurement of PIB binding to brain homogenates obtained post-mortem from patients with AD (8). Aβ peptides were not measured in this study but were interpolated from a different study by Näslund *et al.* (17). The conclusion was a binding stoichiometry approaching 1:1, much higher than all reports based on the direct study of Aβ fibrils *in vitro* (8).

The binding properties of the ligands to Aβ fibrils have all been characterized by using essentially identical filter binding assays employing either narrow ranges of radioligand to determine K_d values (10, 13) or a single fixed low concentration of radioligand and varying concentrations of cold competitor (7, 18). The former assay format will only generally detect very high affinity binding as lower affinity interactions dissociate during the filter washing step, whereas the latter format is a site-specific assay and will not be sensitive to novel ligand-binding sites. The results of these assays have not yet been confirmed by other ligand-binding techniques.

We have addressed these issues by developing a series of homogeneous binding assays that take advantage of the intrinsic fluorescence of both Thio T and a number of representative derivative compounds to measure their binding properties over a wide range of ligand and Aβ fibril concentrations. The results of these assays were compared with classical radioligand binding assays and are consistent with the presence of the previously described low density ligand-binding site but also demonstrate the presence of additional higher density ligand-binding sites on the fibrils. The selectivity of these additional sites and their potential significance for the innovation of selective PET radioligands for the clinical investigation of AD and its treatments are discussed.

MATERIALS AND METHODS

Compound Names and Sources—The structures of the compounds employed in this study are shown in Fig. 1 and are as follows: thioflavin T (Thio T); 2-[4′-(methylamino)phenyl]benzothiazole (BTA-1) (19); 2-[4′-(methylamino)phenyl]-6-methylbenzothiazole (6-Me-BTA-1) (7); 2-(4′-dimethylamino-)phenylimidazo[1,2-*a*]-pyridine (IMPY-H) (9); 6-methyl-2-(4′-dimethylamino-)phenylimidazo[1,2-*a*]-pyridine (IMPY-Me) (9); 2-[4′-(dimethylamino)phenyl]-6-iodobenzothiazole (TZDM) (10); 2-[4′-(4″-methylpiperazin-1-yl)phenyl]-6-iodobenzothiazole (TZPI) (10); and 5-bromo-2-(4-dimethylaminophenyl)benzofuran (BF1) (20). Thio T was obtained from Merck. The remainder of the compounds was custom-synthesized and confirmed for purity by reverse-phase high pressure liquid chromatography, one-dimensional NMR, and mass spectrometer analysis. Radiolabeled 2-[4′-([^{3}H]methylamino)phenyl]-6-methylbenzothiazole ([^{3}H]Me-BTA-1) (84 Ci/mmol, 1 mCi/ml) was custom-synthesized by Amersham Biosciences. All other chemicals were from Sigma with the exceptions of Congo Red and phosphotungstic acid that were obtained from Gee Lawson (London, UK) and Agar Scientific (Stansted, UK).

Preparation of Aβ-(1–40) Fibrils—Human Aβ-(1–40)-peptide (Batch number MK0611 from California Peptide Research, Napa, CA) was incubated at 0.5 mg/ml in PB buffer (10 mM sodium phosphate, 1 mM EDTA, pH 7.4) at 37 °C for 48 h in an orbital shaker at 200 rpm. The formation of fibrils was confirmed by Congo Red binding (21) and Thio T binding (21) together with analysis by negative stain electron microscopy using 1% phosphotungstic acid. Fibrils were used immediately upon production or aliquoted and stored at −80 °C. No difference in ligand binding behavior was observed between freshly prepared and frozen material as noted also by others (7).

Compound Preparation—All compounds were prepared as 1–10 mM Me_2SO stocks before dilution into assay buffer. The maximum final concentration of Me_2SO in the assays was 0.5%. Because of the relatively low solubility of the ligands (with the exception of Thio T) in aqueous solution, all assays were performed in PB supplemented with 10% ethanol (PBE) and at a maximum concentration of 5 μM compound.

Intrinsic Fluorescence Binding Assays—Intrinsic fluorescence intensity (FLINT) changes associated with ligand binding to Aβ-(1–40) were recorded in a Ultra Evolution 384 plate reader (Tecan, Reading, UK) using a 340–440-nm filter pair. For assays measuring the binding of Thio T, a 450–505-nm filter pair was used. Two formats were used for the FLINT assays. FLINT1 was performed using a fixed concentration of ligand (50 or 100 nM) and varying concentrations of Aβ-(1–40) polymer. FLINT2 was performed using a fixed concentration of Aβ-(1–40) (500 nM) and varying concentrations of ligand (0 to 2 μM) as detailed under "Results."

Fluorescence polarization measurements were recorded in a Ultra Evolution 384 plate reader using a 360-nm polarizing excitation filter and 440-nm emission filters. The assays employed a fixed concentration of BTA-1 (50 nM) and varying concentrations of Aβ-(1–40) (0–50 μM).

All fluorescent assays were performed in PBE in a final volume of 80 μl and were incubated for 2 h at 20 °C before reading. All data points were performed at least in quadruplicate and were analyzed using Grafit (Erithacus Software Limited, Horley, UK) to obtain K_d values using the single site ligand-binding module.

Fluorescence Competition Assays (FLINT3)—Competition assays employed a fixed concentration of Aβ-(1–40) (2 μM) and Thio T (1 μM) and used varying concentration ranges of competitor ligands (up to 4 μM). Reactions were performed in PBE in a final volume of 80 μl and were incubated for 2 h at 20 °C before measurement in a Ultra Evolution 384 plate reader using a 450–505-nm filter pair. All data points were performed in quadruplicate, and the fluorescent signal in the absence of competitor defined a fractional binding of 1. Data were analyzed using Grafit to obtain IC_{50} values using full 4-parameter curve fits. K_i values were derived from the Cheng-Prusoff equation (22), $K_i = IC_{50}/(1 + ([L]/K_d))$ were [L] was the concentration (1000 nM) and K_d (750 nM) of Thio T used in the assay.

Fluorescence Energy Transfer (FRET) Measurements—FRET assays employed fixed concentrations of Aβ-(1–40) (2 μM) and Thio T (1 μM) and either 100 nM BF1 or 100 nM BTA-1 in PBE. Measurements were performed in a RF-5301PC spectrofluorimeter (Shimadzu Europa, Milton Keynes, UK) running Hyper RF software. Emission spectra (400–550 nm) were collected following excitation at 340 nm using excitation and emission slit widths of 5 and 1.5 nm, respectively.

Radioligand Binding Assays—A fixed concentration of Aβ-(1–40) (40 nM) was titrated against a range of [^{3}H]Me-BTA-1 concentrations (0.05–40 nM) in PB buffer supplemented with 10% ethanol (PBE) for 3 h at 20 °C. The final reaction volume was 500 μl. Nonspecific binding was determined in the presence of 50 μM Thio T. The bound and free fractions were separated by vacuum filtration through GF/B glass filters (Whatman, Maidstone, UK) using an M-48T harvester (Brandel, Gaithersburg, MD) followed by four 1-ml washes with PBE. Filters containing the bound ligand were mixed with 3 ml of Ultima Gold MV scintillation liquid (PerkinElmer Life Sciences) and incubated for 2 h before counting in a TriCarb 2100TR liquid scintillation counter (PerkinElmer Life Sciences). All data points were performed in triplicate. The specific binding signal under these assay conditions was ~70%. Data were analyzed using Grafit to obtain the apparent dissociation constant (K_d) and the maximal number of binding sites (B_{max}) using the single site ligand-binding module.

Radioligand Competition Assays—Competition assays employed a fixed concentration of Aβ-(1–40) (40 nM) and [^{3}H]Me-BTA-1 (4 nM) and used varying concentration ranges of cold competitor dependent on the ligand. Reactions were performed in PBE and were incubated for 2 h at 20 °C before harvesting and counting as described above. Nonspecific binding was determined in the presence of 50 μM Thio T. BF1 (200 nM) was used to determine nonspecific binding for assays involving Thio T. All data points were performed in triplicate, and the specific binding signal in the absence of competitor defined a fractional binding of 1. Data were analyzed using Grafit to obtain IC_{50} values using full 4-parameter curve fits. K_i values were derived as stated above using the Cheng-Prusoff equation (22), where [L] was the concentration (4 nM) and K_d (4.2 nM) of the radioligand used in the assays.

Density Gradient Centrifugation of Aβ Fibrils—Aβ fibril preparations were fractionated on gradients consisting of 700 μl each of 60, 50, 40, 30, 20, 10, and 280 μl of 5% Optiprep (Sigma) prepared in 13 × 51-mm ultraclear centrifuge tubes (Beckman Instruments, High Wycombe, UK). A 300-μl sample of Aβ fibrils (0.5 mg/ml) in PB was carefully layered on top of the Optiprep gradient and then fractionated at 50,000 rpm for 2 h and 30 min at 22 °C in an Optima Max-E ultracentrifuge using an MLS-50 swinging bucket rotor (Beckman Instruments). Following centrifugation, the bottoms of the tubes were

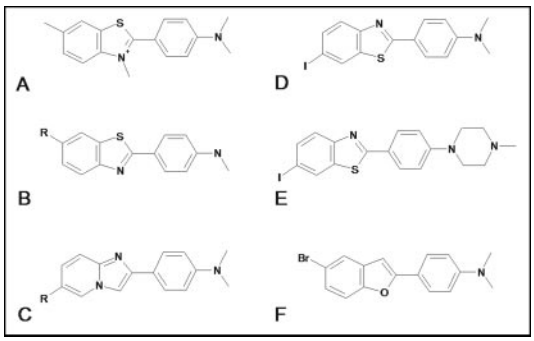

FIG. 1. **Compound structures.** *A*, Thio T; *B*, BTA, *R*=H (BTA-1)/CH_3 (6Me-BTA-1); *C*, IMPY, *R*=H (IMPY-H)/CH_3 (IMPY-Me); *D*, TZDM; *E*, TZPI; and *F*, BF1. Full compound nomenclatures are provided under "Compound Names and Sources."

pierced with a 21-gauge syringe needle, and 12 × 400-μl fractions were collected for analysis. Fraction 1 represents the most dense part of the gradient and fraction 12 the least dense part of the gradient.

The fractions were analyzed for thioflavin T binding by mixing 80 μl of each fraction with 2 μl of 100 μM thioflavin and reading the fluorescence after 2 h of incubation in an Ultra Evolution 384 plate reader using a 450–505-nm filter pair. In addition, 5 μl of each fraction was separated by SDS-PAGE followed by blotting onto nitrocellulose as described previously (23). Blots were probed with the mouse anti-human β-amyloid antibody 6E10 (Merck) at a 1:1000 dilution followed by an anti-mouse horseradish peroxidase-conjugated antibody (Sigma) at a 1:10,000 and were then developed with SuperSignal West Dura extended duration substrate (Perbio, Cheshire, UK). Images of the blot were captured using a Chemigenius2 imaging system (Syngene, Cambridge, UK) and quantified using Genetools (Syngene). Radioligand binding was evaluated by mixing 50 μl of each fraction with 450 μl of 4 nM [^{3}H]Me-BTA-1 prepared in PBE. The reactions were incubated for 2 h at 20 °C before harvesting and counting as described above by vacuum filtration.

RESULTS

Determination of Binding Constants Using Fluorescence Assays—The compounds used in this study (Fig. 1) all share similar fluorescent properties, with excitation and emission wavelengths of around 340 and 440 nm, respectively, but that are distinct from those of Thio T (450:480 nm) (data not shown). In addition, the compounds display increases in their intrinsic FLINT when bound to Aβ-(1–40) fibrils along with slight shifts in their excitation and emission wavelengths consistent with ligand binding into a hydrophobic pocket on the fibrils. The exception to this was BTA-1, which displayed a slight decrease (~5–10%) in FLINT when bound to the Aβ-(1–40) fibrils.

The increases in FLINT upon ligand binding to Aβ-(1–40) fibrils were exploited in designing simple, homogeneous assays to directly measure compound binding. Two assay formats were employed, FLINT1 and FLINT2. In FLINT1 assays, compound binding was measured by using a fixed concentration of ligand (50 or 100 nM) and varying concentrations of Aβ-(1–40) polymer (Fig. 2, *A* and *C*). A fixed concentration of Aβ-(1–40) polymer (500 nM) and varying concentrations of ligand were used in the FLINT2 assays (Fig. 2, *B* and *D*). The binding constants K_{d1} and K_{d2} obtained from the FLINT1 and FLINT2 assays are summarized in Table I.

The binding of BTA-1 to Aβ-(1–40) fibrils was determined by fluorescent anisotropy measurements using a fixed concentration of ligand (50 nM) and varying concentrations of polymer (Fig. 2*E*). The apparent K_d value from this assay was 5.23 μM. The anisotropy value of the compound at saturating concentrations of polymer was 0.4, which is toward the maximum limit for a fluorophore (24) and probably reflects the large Stokes radii of the Aβ-(1–40) polymers.

The binding isotherms for all of the ligands in all assay formats were consistent with a single population of binding sites for each of the ligands. The apparent K_d values from the assays were found to be strongly dependent on the assay format, with the FLINT2 assays consistently reporting lower values. In addition, the rank order of binding constants for the individual compounds was conserved between the two assay formats (Table I).

Comparison of the K_{d2} values with the literature values obtained previously indicates that although fluorescence assays are reporting significantly higher values, the rank order of binding affinities is generally well conserved. The exception to this was Thio T whose K_{d2} value was essentially identical to that reported using a similar assay format by Naiki *et al.* (25) and LeVine (26), indicating that the present set of assays was accurately reporting binding constants.

Comparison of Binding Constants Is Consistent with Two Classes of Binding Sites on the Aβ Fibrils—The observation that the binding constants were dependent on assay format was unexpected as both assay formats should report approximately the same K_d values. However, an explanation for this difference became apparent when the number of potential binding sites on the Aβ polymer was considered. The binding data previously reported with these ligands demonstrated that the binding site density on the Aβ fibrils was $\ll$1 site per Aβ peptide monomer (8, 14). This meant that the effective concentration of binding sites on the fibrils was potentially significantly less than the concentration of Aβ peptide monomers added to the FLINT1 assay. Because calculation of the K_{d1} values are based on the Aβ peptide monomer concentration, this leads to an overestimation of the binding constant by a factor dependent on the binding site density. In contrast, the calculation of K_{d2} values is directly dependent on the ligand concentration, and as a consequence the FLINT2 assay does not overestimate the binding constants.

Furthermore, the ratio K_{d1}/K_{d2} allows an estimation of the ligand-binding site density on the Aβ-(1–40) fibrils (Table I). This sum clearly splits the ligands into two distinct groups. Thio T, IMPY-H, and IMPY-Me have a ratio of ~30–40 (*i.e.* 1 ligand-binding site per ~35 Aβ-(1–40) monomers), whereas TZDM, TZPI, and BF1 have a ratio of ~3–5 (*i.e.* 1 ligand-binding site per ~4 Aβ-(1–40) monomers). These data suggested that there were at least two distinguishable classes of binding sites on the Aβ fibrils and are supported by the observation that the latter group of compounds all contain a halogen substitute on their aromatic ring.

In summary, the data from the intrinsic fluorescence assays are as follows: (*a*) consistent with a single affinity binding mode for each ligand and accurately reporting intrinsic binding constants; (*b*) determining K_d values significantly higher than that previously described; and (*c*) when combined with the evidence of the binding site densities and selectivity the data, suggested that there was more than one class of binding site on the Aβ fibrils: a low density site (every ~35 Aβ monomers) and a higher density site (every ~4 Aβ monomers) that are termed BS1 and BS2, respectively.

Fluorescent Competition Assays Support Presence of BS1 and BS2—Ligand binding to Aβ-(1–40) fibrils was further characterized by using a fluorescent competition assay (FLINT3) employing Thio T as a reporter for BS1. The K_i values obtained from these assays were again significantly higher than those reported in the literature (Table I). However, they were similar to the K_{d2} values providing additional evidence that the fluorescent assays were accurately reporting binding data and consistent with our thesis that there were additional ligand-binding sites on the Aβ fibrils.

The competitive binding curves were consistent with displacement from a single type of site for each ligand on the

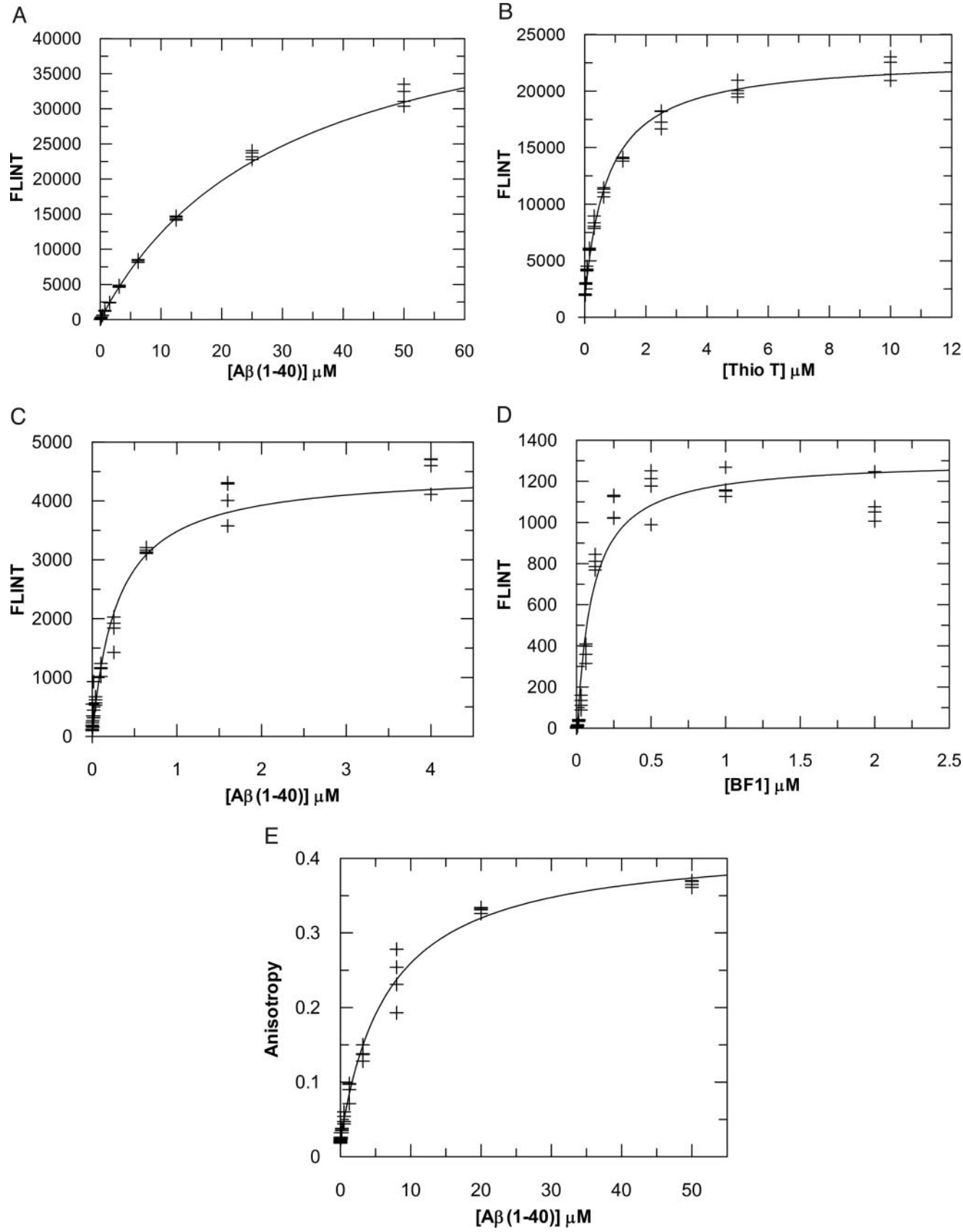

FIG. 2. **Fluorescence ligand binding assays.** *A* and *C* are shown in FLINT1 assay format; *B* and *D* are in FLINT2 assay format; and *E* is a fluorescence anisotropy assay. Representative binding isotherms for Thio T (*A* and *B*), BF1 (*C* and *D*), and BTA-1 (*E*) are shown.

fibrils (Fig. 3) and also indicated that the compounds could again be separated into the same two groups identified from the FLINT1/2 assays such that IMPY-H and IMPY-Me (and BTA-1) were able to displace >80% of the bound Thio T (Fig. 3*A*), whereas TZDM, TZPI, and BF1 were able to displace <50% of the bound Thio T (Fig. 3*B*). Full displacement curves

TABLE I
Summary of fluorescent and radioligand (RL) binding data

K_d values are shown in boldface. The K_i values for both IMPY derivatives in the Thio T competition assay have not been calculated due to their limited solubility in aqueous solution resulting in incomplete displacement curves. RLA, radioligand assay using [^{3}H]Me-BTA-1. Literature values are shown for comparison in the last column. ND, not determined; NA, not applicable.

Compound	FLINT1 K_{d1}	FLINT2 K_{d2}	Ratio K_d1/K_d2	FLINT3 K_i	RLA K_d/K_i	Literature K_d/K_i
	nM			*nM*	*nM*	*nM*
Thio T	**30,350**	**750**	40.5	NA	1610	**760**[24], **2000**[25]
[^{3}H]Me-BTA-1	ND	ND	ND	ND	**4.2**	20.2[7a]
BTA-1	**5230**	ND	ND	200	19.5	**2.8**[8]
IMPY-H[b]	**43,410**[b]	**1420**	30.6	>1000	142	1242[9]
IMPY-Me	**35,560**	**1000**	35.6	>1000	42	242[9]
TZDM	**430**	**120**	3.6	145	2.8	**0.06**[10]
TZPI	**870**	**170**	5.1	480	6.2	**0.13**[10]
BF1	**300**	**120**	2.5	110	3	1.6[20]

[a] IC_{50} value is indicated.
[b] Note that the standard errors were all <10% of calculated values, with the exception of IMPY-H.

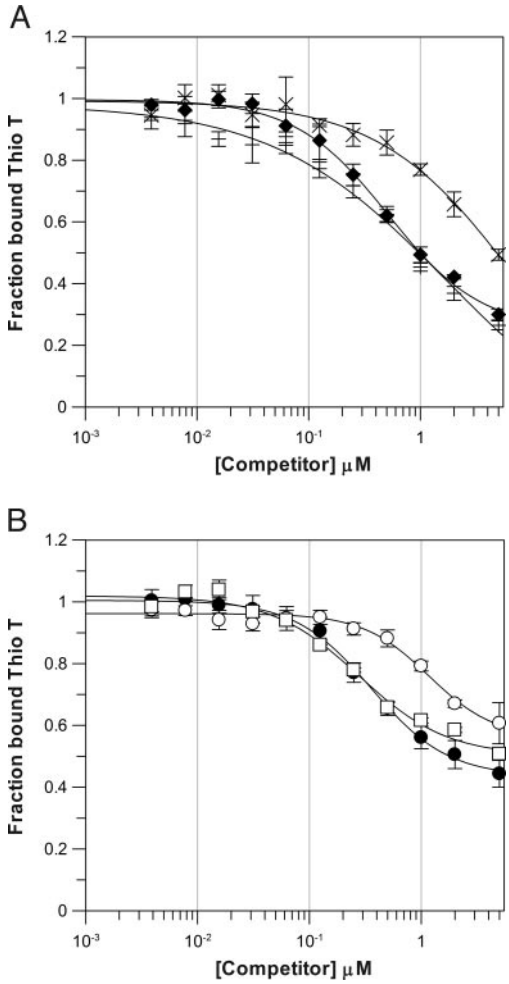

FIG. 3. **Fluorescent competition assays.** Dose-response curves showing the fractional binding of Thio T to Aβ-(1–40) fibrils in the presence of competitor ligands. *A,* ♦, BTA-1; +, IMPY-Me; ×, IMPY-H. *B,* ○, TZDM; ●, TZPI; □, BF1.

for the IMPY ligands could not be accurately obtained due to compound insolubility at higher concentrations, but it is apparent that they are displacing >50% of the Thio T and that their K_i values are consistent with their K_{d2} values. The ability of the ligands TZDM, TZPI, and BF1 to partially displace Thio T may be a consequence of the spatial arrangement of higher density BS2 relative to BS1 on the Aβ fibrils such that they periodically either partially or completely overlap with BS1.

FRET Measurements Indicate That BS1 and BS2 Are Independent Sites on the Aβ Fibril—Further supporting evidence for the spatial separation but close proximity of BS1 and BS2 was obtained from fluorescent resonance energy transfer (FRET) measurements. The differing fluorescent properties of BF1 (BS2 probe, excitation/emission maxima 340:440 nm) and Thio T (BS1 probe, excitation/emission maxima 450:480 nm) were again exploited, but this time as a potential donor-acceptor pair.

By using an excitation wavelength of 340 nm, which specifically excites BF1, the emission spectra of Aβ-(1–40) fibrils incubated with either Thio T or Thio T/BF1 were recorded. Calculation of the difference spectrum between the samples demonstrated the presence of an emission maximum at ~480 nm, corresponding to the expected wavelength for the Thio T emission (Fig. 4). This experiment was repeated by replacing BF1 with BTA-1, which has similar excitation/emission maxima but should directly compete with Thio T for BS1. No fluorescent signal was observed at 480 nm with the BTA-1. These data clearly demonstrate that only BF1 is able to efficiently transfer energy to Thio T consistent with BS1 and BS2 representing spatially independent ligand-binding sites on the Aβ fibrils.

Radioligand Assays Indicate a Third Class of Binding Site on the Aβ Fibrils—In order to ascertain whether the observed differences in binding affinities between the literature and fluorescent assays reported here were because of the different assay formats, the binding of [^{3}H]Me-BTA-1 to Aβ-(1–40) fibrils was determined by using a filter binding assay. The resulting binding isotherm was consistent with the presence of a single high affinity binding site on the polymer with an apparent K_d of 4.2 nM and a maximal binding (B_{max}) of 0.13 when measured at 40 nM Aβ monomer concentration (Fig. 5*A*). The K_d value is slightly higher than the previously reported IC_{50} value for this compound of 20 nM (7); and the low B_{max} value, equating to ~1 ligand-binding site per 300 Aβ-(1–40) monomers, is consistent with that found for other similar compounds such as 6-OH-BTA-1/PIB and BTA-1 (8).

The data from this set of experiments were consistent with the identification of the previously described very low density site on Aβ-(1–40) fibrils. Given that the ligand-binding characteristics of this site were clearly differentiated from BS1 and BS2, it is suggested that this represents a third class of binding site, termed BS3.

In competitive binding assays, all of the ligands tested were able to displace [^{3}H]Me-BTA-1 in a manner consistent with a single class of binding sites on the Aβ fibril (Fig. 5*B*). The K_i values derived from these assays were significantly lower than the values derived from both the FLINT2 and Thio T fluorescent competition assays. However, again the relative order of binding affinities was conserved between the radioligand and fluorescent assays (Table I).

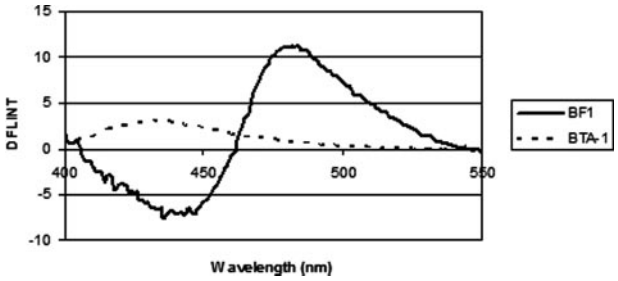

FIG. 4. **Evidence of FRET between BS1 and BS2.** Difference emission spectra (*DFLINT*) following excitation at 340 nm of Aβ-(1–40) fibrils incubated with Thio T and either BF1 or BTA-1. Only in the presence of BF1 is there a fluorescent signal at the expected emission wavelength of Thio T (~480 nm) indicative of energy transfer between the two fluorophores.

In addition, the radioligand competition assays have allowed a direct comparison, under a standard set of conditions, of ligand binding to this low density site on the Aβ-(1–40) fibrils. The K_i values from the current set of experiments are broadly in agreement with the previously published values for these compounds both in terms of potency and rank order of binding affinity.

The inability to detect ligand binding at BS3 by using fluorescent techniques may be due to a number of related factors. The relative contribution of this site to a binding signal (whether FLINT or anisotropy) would be small relative to the more densely packed BS1 and BS2. By assuming that a ligand produced an identical FLINT increase when bound to any of the sites, the observed signal from BS3 would be a tenth or a hundredth smaller than that observed at BS1 and BS2, respectively. In addition, it is possible that ligand binding to BS3 may significantly quench or produce no change in ligand fluorescence making it difficult to detect by either FLINT or anisotropy measurements.

Evidence That BS1, BS2, and BS3 Are Uniformly Distributed on the Aβ Fibrils—Although the FRET data were able to demonstrate that BS1 and BS2 were in close proximity on the same Aβ fibril, the radioligand data do not directly imply that BS3 is also distributed on the same population of fibrils. To address this issue, we separated the Aβ fibrils by density gradient ultracentrifugation using a method adapted from Ward *et al*. (27), and we assayed the resulting fractions for Aβ immunoreactivity and thioflavin T and [^{3}H]Me-BTA-1 binding (Fig. 6).

Based on the immunoreactivity of the anti-Aβ antibody 6E10, the centrifugation step split the fibrillar preparation into two peaks centered on fractions 3 and 5. The vast majority (~80%) of the signal from the blot is present in fraction 3, and this is consistent with the expected high molecular mass of the Aβ fibrils and similar to that found previously using this method (27). Fraction 5 is a small shoulder on the main peak of Aβ immunoreactivity indicative of a second population of high molecular mass species in the fibrillar preparation, although of lesser mass than fraction 3.

The ligand binding properties of both Thio T (BS1 probe) and [^{3}H]Me-BTA-1 (BS3 probe) to these fractions display an identical pattern both to each other and also to the signal obtained from the Aβ immunoblot. These findings support the idea that the ligand-binding sites are uniformly distributed across the Aβ fibril preparation and are not restricted to morphologically distinct subpopulations of polymers.

DISCUSSION

The development of potentially useful PET ligands for the detection of SPs is being widely pursued because of the clinical importance such imaging would have (6). However, until now, the binding properties of these prospective PET ligands to Aβ fibrils have not been rigorously examined, raising doubts over the true significance of the clinical investigations performed to date. We have developed and performed a range of assays that, for the first time, have allowed a full analysis of the binding of a series of Thio T derivatives to Aβ-(1–40) fibrils *in vitro*. Our data are consistent with the presence of a previously described binding site (BS3) to which all of the compounds bind with high affinity, but it also demonstrates the presence of two additional high affinity and much more abundant binding sites (BS1 and BS2). The finding of these additional binding sites on the Aβ-(1–40) fibrils may help resolve issues surrounding the nature of the signal detected *in vivo* by PET with these ligands.

A number of lines of evidence support the presence of multiple ligand-binding sites on the Aβ-(1–40) polymers. First, both the K_d and K_i values from two independent fluorescence-based assay formats are significantly higher than the values reported from previous and the currently described radioligand binding assays. This provides direct evidence of additional li-

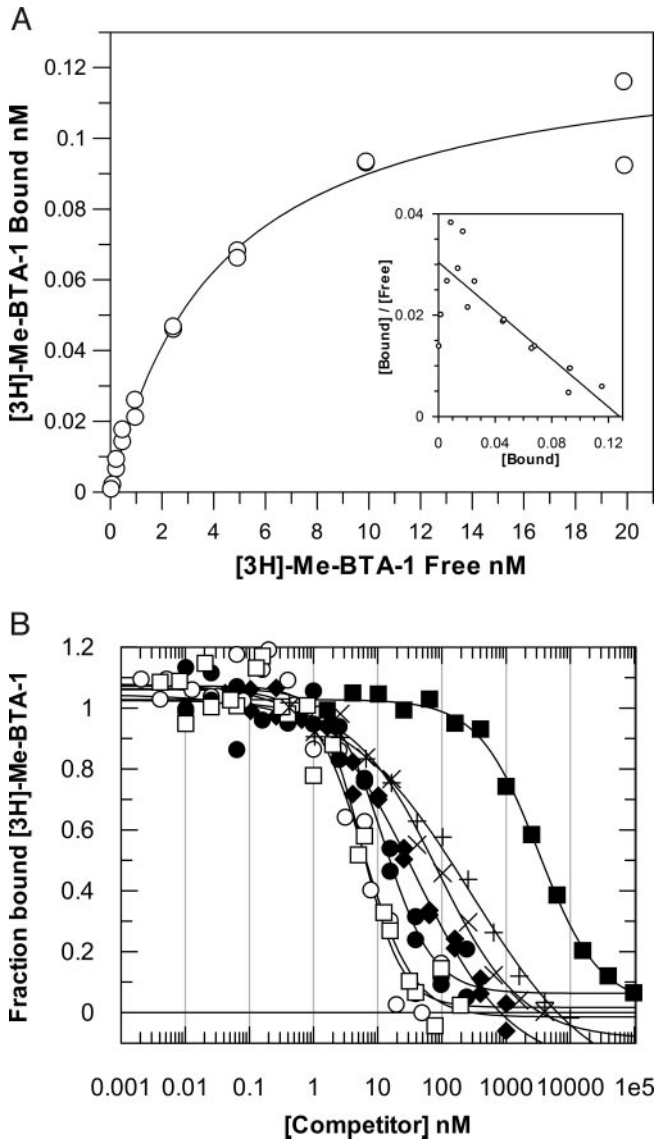

FIG. 5. *A*, binding isotherm for the ligand [^{3}H]Me-BTA-1 with Aβ-(1–40) fibrils. Scatchard analysis is shown in the *inset*. The K_d and B_{max} values derived from this analysis were 4.2 and 0.13 nM, respectively. *B*, radioligand competition assays. Dose-response curves showing the fractional binding of [^{3}H]Me-BTA-1 to Aβ-(1–40) fibrils in the presence of competitor ligands: ■, Thio T; ×, IMPY-H; +, IMPY-Me; □, BF1; ○, TZDM; ●, TZPI; ♦, BTA-1. The standard deviations for all points were <10% and are not plotted for clarity.

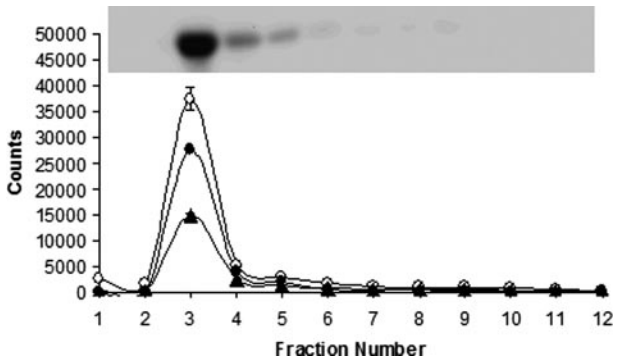

FIG. 6. **Analysis of fractions from the density gradient centrifugation of Aβ fibrils.** ○, TT fluorescence (arbitrary units); ●, 6E10 immunoreactivity (arbitrary units); ▲, [^{3}H]Me-BTA-1 dpm (×10). *Inset* shows a blot of the fractions using the 6E10 antibody. Note that fraction 1 contains the most dense material and fraction 12 the least dense material.

gand-binding sites on the Aβ-(1–40) fibrils. In addition, the FLINT assays also demonstrated that the binding site densities of BS1 and BS2 are significantly higher than that of BS3.

Finally, the selectivity of compounds containing a halogen substitution on their aromatic ring systems (TZDM/TZPI/BF1) provides a structural discriminator for BS1 and BS2. The ability of BS3 to accommodate both halogen- and nonhalogen-containing structures suggests a hybrid-binding site that occurs periodically only when BS1 and BS2 are in complete register on the fibril. However, the significantly different binding constants for ligands between BS1/2 and BS3 would argue that the latter site is a spatially distinct periodic feature of the polymer. A schematic demonstrating the potential arrangement of binding sites on the Aβ-(1–40) fibril is shown in Fig. 7. This model proposes that all three types of binding sites are present together on the majority of Aβ fibrils in the polymerized mixture and takes into account the FRET data demonstrating the close spatial proximity of BS1 and BS2 and the congruent distribution of fluorescence and radioligand-binding sites following fractionation of polymers by density gradient centrifugation.

A high resolution structure of amyloid fibrils formed from Aβ peptides is not available, making it difficult to associate the ligand-binding sites with structural features on the polymer. The increase in the intrinsic fluorescence of the ligands is indicative of compound binding into a hydrophobic pocket on the polymer and suggests that BS1 and BS2 are associated with the two hydrophobic clusters (residues 17–21 and 30–40) on the Aβ peptide (reviewed in Ref. 28).

The presence of multiple classes of binding sites on the Aβ fibrils is also supported by two studies using the ligand FDDNP. The first study using a radioligand filter binding assay indicated that [18F]FDDNP was not displaceable by Thio T from Aβ-(1–40) fibrils (29). However, a recent study (30) demonstrated that, in a fluorescent competition assay using Thio T and Aβ-(1–40) fibrils (in an essentially identical format to that described here), FDDNP was able to displace Thio T. These findings are consistent with the presence of both independent and common/overlapping binding sites on the fibrils.

The increase in the intrinsic fluorescence of Thio T has been exploited through its use as a histological dye in the post-mortem diagnosis of AD (31, 32). Our findings would suggest that the signal obtained in the post-mortem tissue is primarily associated with its interaction with BS1 and would also suggest that the fluorescent signal associated with the use of these Thio T derivatives in histological studies, when the compounds are used at relatively high concentrations (>100 nM), is not from BS3 but primarily from the large increase in FLINT associated with the higher density BS1 and BS2.

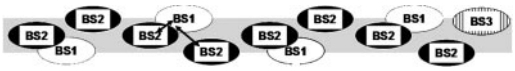

FIG. 7. **A model of binding sites on Aβ fibrils for the Thio T class of ligands.** BS3 is the previously described independent low density site. BS1 and BS2 are the newly identified higher density sites that are independent from BS3. The arrangement of BS1 and BS2 schematically reflects how differences in their relative polymer density can lead to the sites periodically occurring in close proximity and/or partially overlapping. The *short* and *long arrows* indicate how both displacement and FRET can occur between BS1 and BS2, respectively.

An approximate rule for the success of a radioligand in *in vivo* imaging experiments makes use of the term binding potential (BP) which is the sum of B_{max}/K_d; values >10 generally produce a sufficient signal for PET studies (8). The *in vivo* value of B_{max} necessary for the calculation of the BP has not been determined, however, Näslund *et al.* (17) have calculated the regional distribution of total Aβ-(1–40) and Aβ-(1–42) levels (soluble and plaque) in formic acid extracts of post-mortem brains from both control and AD cohorts. Their findings suggest that levels of total Aβ load approached 1–3 μM in the cortical regions of AD brains. By using the mid-point of the data set together with the K_d of 4.2 nM for [^{3}H]Me-BTA-1, a BP of ~500 is obtained. However, when the *in vitro* binding stoichiometry of the radioligand binding to BS3 is taken into account, the BP is reduced to ~2, which is unlikely to generate a significant PET signal *in vivo*. Although higher B_{max} values have been reported for BTA-1 and PIB binding to AD brain homogenates, the levels of Aβ peptides in this study were not explicitly measured (8).

One key question that arises from the present set of studies is as follows: what might be relative potential contributions of BS1 and BS2 compared with BS3 in the signal obtained from a PET study? Using BTA-1 (K_i 200 nM), BF1 (K_d 110 nM), and Me-BTA-1 (K_d 4.2 nM) as model compounds for BS1, BS2, and BS3 and taking into account the stoichiometry of these sites (1:35, 1:4, and 1:300), the levels of Aβ peptides required to produce a BP of 10 are 70, 4, and 12 μM respectively. The values for all of the compounds are clearly at the top end of the reported concentrations for Aβ peptides but suggest that BS2 may make a more significant contribution than BS1 and potentially BS3 to the observed PET signals.

These data also suggest that the design of higher affinity compounds targeting BS2 may result in improved PET ligands for imaging plaque deposits. In addition, the radioligand assays currently widely in use for compound screening and selection may be targeting the "wrong" site on the fibrils, the low density BS3, and that fluorescence-based screens, such as those using Thio T, may identify compounds with more desirable properties for *in vivo* imaging studies.

In conclusion, our data support a complex model for the binding of PET radioligands being designed for tracking SPs in AD, with the presence of multiple ligand-binding sites on Aβ fibrils. The development of therapy for AD is presently hampered by the fact that there is no sensitive test of the progression and regression of the underlying pathology before cognition is affected (6). Understanding the properties of Aβ fibrils will assist in the more rational design of more effective specific PET radioligands to track the progression of this disease and accelerate the development of treatments.

Acknowledgments—We thank Christine Parker and Gill Brown for help with the radioligand binding assay and electron microscopy and David Powell and David Howlett for helpful discussions.

REFERENCES

1. Vickers, J. C., Dickson, T. C., Adlard, P. A., Saunders, H. L., King, C. E., and McCormack, G. (2000) *Prog. Neurobiol.* **60,** 139–165
2. Selkoe, D. J., and Schenk, D. (2003) *Annu. Rev. Pharmacol. Toxicol.* **43,** 545–584

3. Tolnay, M., and Probst, A. (2003) *IUBMB. Life* **55,** 299–305
4. Braak, H., and Braak, E. (1991) *Acta Neuropathol.* **82,** 239–259
5. Gold, G., Kovari, E., Corte, G., Herrmann, F. R., Canuto, A., Bussiere, T., Hof, P. R., Bouras, C., and Giannakopoulos, P. (2001) *J. Neuropathol. Exp. Neurol.* **60,** 946–952
6. Nordberg, A. (2004) *Lancet Neurol.* **3,** 519–527
7. Klunk, W. E., Wang, Y., Huang, G. F., Debnath, M. L., Holt, D. P., and Mathis, C. A. (2001) *Life Sci.* **69,** 1471–1484
8. Mathis, C. A., Wang, Y., Holt, D. P., Huang, G. F., Debnath, M. L., and Klunk, W. E. (2003) *J. Med. Chem.* **46,** 2740–2754
9. Kung, M. P., Hou, C., Zhuang, Z. P., Zhang, B., Skovronsky, D., Trojanowski, J. Q., Lee, V. M., and Kung, H. F. (2002) *Brain Res.* **956,** 202–210
10. Zhuang, Z. P., Kung, M. P., Hou, C., Skovronsky, D. M., Gur, T. L., Plossl, K., Trojanowski, J. Q., Lee, V. M., and Kung, H. F. (2001) *J. Med. Chem.* **44,** 1905–1914
11. Styren, S. D., Hamilton, R. L., Styren, G. C., and Klunk, W. E. (2000) *J. Histochem. Cytochem.* **48,** 1223–1232
12. Klunk, W. E., Bacskai, B. J., Mathis, C. A., Kajdasz, S. T., McLellan, M. E., Frosch, M. P., Debnath, M. L., Holt, D. P., Wang, Y., and Hyman, B. T. (2002) *J. Neuropathol. Exp. Neurol.* **61,** 797–805
13. Kung, H. F., Lee, C. W., Zhuang, Z. P., Kung, M. P., Hou, C., and Plossl, K. (2001) *J. Am. Chem. Soc.* **123,** 12740–12741
14. Agdeppa, E. D., Kepe, V., Liu, J., Flores-Torres, S., Satyamurthy, N., Petric, A., Cole, G. M., Small, G. W., Huang, S. C., and Barrio, J. R. (2001) *J. Neurosci.* **21,** 189
15. Klunk, W. E., Engler, H., Nordberg, A., Wang, Y., Blomqvist, G., Holt, D. P., Bergstrom, M., Savitcheva, I., Huang, G. F., Estrada, S., Ausen, B., Debnath, M. L., Barletta, J., Price, J. C., Sandell, J., Lopresti, B. J., Wall, A., Koivisto, P., Antoni, G., Mathis, C. A., and Langstrom, B. (2004) *Ann. Neurol.* **55,** 306–319
16. Small, G. W., Agdeppa, E. D., Kepe, V., Satyamurthy, N., Huang, S. C., and Barrio, J. R. (2002) *J. Mol. Neurosci.* **19,** 323–327
17. Naslund, J., Haroutunian, V., Mohs, R., Davis, K. L., Davies, P., Greengard, P., and Buxbaum, J. D. (2000) *J. Am. Med. Assoc.* **283,** 1571–1577
18. Kung, H. F., Kung, M. P., Zhuang, Z. P., Hou, C., Lee, C. W., Plossl, K., Zhuang, B., Skovronsky, D. M., Lee, V. M., and Trojanowski, J. Q. (2003) *Mol. Imaging Biol.* **5,** 418–426
19. Mathis, C. A., Bacskai, B. J., Kajdasz, S. T., McLellan, M. E., Frosch, M. P., Hyman, B. T., Holt, D. P., Wang, Y., Huang, G. F., Debnath, M. L., and Klunk, W. E. (2002) *Bioorg. Med. Chem. Lett.* **12,** 295–298
20. Ono, M., Kung, M. P., Hou, C., and Kung, H. F. (2002) *Nucl. Med. Biol.* **29,** 633–642
21. Nilsson, M. R. (2004) *Methods* (*Orlando*) **34,** 151–160
22. Cheng, Y., and Prusoff, W. H. (1973) *Biochem. Pharmacol.* **22,** 3099–3108
23. Hong, G., Lockhart, A., Davis, B., Rahmoune, H., Baker, S., Ye, L., Thompson, P., Shou, Y., O'Shaughnessy, K., Ronco, P., and Brown, J. (2003) *FASEB J.* **17,** 1966–1968
24. Pope, A. J., Haupts, U. M., and Moore, K. J. (1999) *Drug Discov. Today* **4,** 350–362
25. Naiki, H., Higuchi, K., Hosokawa, M., and Takeda, T. (1989) *Anal. Biochem.* **177,** 244–249
26. LeVine, H., III (1993) *Protein Sci.* **2,** 404–410
27. Ward, R. V., Jennings, K. H., Jepras, R., Neville, W., Owen, D. E., Hawkins, J., Christie, G., Davis, J. B., George, A., Karran, E. H., and Howlett, D. R. (2000) *Biochem. J.* **348,** 137–144
28. Serpell, L. C. (2000) *Biochim. Biophys. Acta* **1502,** 16–30
29. Agdeppa, E. D., Kepe, V., Petri, A., Satyamurthy, N., Liu, J., Huang, S. C., Small, G. W., Cole, G. M., and Barrio, J. R. (2003) *Neuroscience* **117,** 723–730
30. Suemoto, T., Okamura, N., Shiomitsu, T., Suzuki, M., Shimadzu, H., Akatsu, H., Yamamoto, T., Kudo, Y., and Sawada, T. (2004) *Neurosci. Res.* **48,** 65–74
31. Vassar, P. S., and Culling, C. F. (1959) *Arch. Pathol.* **68,** 487–498
32. Kelenyi, G. (1967) *J. Histochem. Cytochem.* **15,** 172–180